

International Journal of Engineering

Journal Homepage: www.ije.irSynthesis and Characterization of Nanocrystalline Ni₃Al Intermetallic during Mechanical Alloying Process

R. Yazdani-rad, M. B. Rahaei*, A. Kazemzadeh, M. R. Hasanzadeh

Materials and Energy Research Center, Tehran, Iran

ARTICLE INFO

Article history:

Received 5 March 2011

Received in revised form 5 February 2012

Accepted 19 April 2012

Keywords:

Ni₃Al

Mechanical alloying

Structural evolutions

Nanostructure

XRD

Rietveld refinement

TEM

A B S T R A C T

In this research, the formation of nanocrystalline Ni₃Al intermetallic from Ni and Al elemental powders by mechanical alloying (MA) process and its characterization was investigated. Therefore, the evolutions in microstructure such as phase transformation, oxidation in air and introduction of Fe impurity from milling media after MA were evaluated using XRD, Rietveld refinement, TEM, SEM, EDS and ICP analyses. Milling after 4 h resulted in formation of Ni₃Al/Al₂O₃ composite in air while continuing milling time up to 8 h resulted in obtaining Ni₃Al product. TEM observations along with XRD combined Rietveld's refinement analysis confirmed obtaining a disorder structure and nanocrystals of Ni₃Al embedded in an amorphous matrix after 16 h milling. Moreover, the lattice parameter of Ni₃Al product and Fe contamination of powder were increased by increasing milling time.

doi: 10.5829/idosi.ije.2012.25.02c.01

1. INTRODUCTION

Numerous alloys based upon Ni₃Al have been developed with broad utilizations ranging from furnace rolls and radiant burner tubes for steel production to heat treating fixtures for carburizing and air environments and corrosion-resistant parts for chemical industries [1-5]. This is because strong bonding between aluminum and nickel, which persists at elevated temperatures, yields excellent properties competitive with those of superalloys and ceramics, such as high melting point, low densities, high strength, as well as good corrosion and oxidation resistance [2,3,5]. But, Ni₃Al intermetallic has not enough strength and hardness for high temperature applications [1].

Nanocrystalline materials are potentially attractive for many applications since the reduction of the grain size to the nanometer scale can improve their physical and mechanical properties. In particular, high strength and hardness or ductilisation of brittle materials superior to conventional materials may be obtained [6,7].

Mechanical alloying (MA) is a rapidly developing technology capable of producing a variety of materials, such as compounds, metastable solid solutions, amorphous alloys, nanocrystalline materials, etc. [6].

The materials processing is very simple and appears to be readily scalable: powders of new materials are produced by high-energy ball milling of starting ingredients. MA offers a number of advantages for processing intermetallic compounds including grain refinement and the formation of fine dispersoid particles [8,9]. The main premise of MA is that during mechanical alloying a solid state reaction takes place between the fresh powder surfaces of the reactant materials at room temperature. Consequently, it can produce alloys and compounds at room temperature, the condition which is difficult or impossible to be applied to conventional melting and casting techniques [8,10]. Furthermore, nanocrystalline structure obtained by milling can improve ductility of intermetallics [6,7].

The synthesis of the nanocrystalline Ni₃Al intermetallic by MA from Ni and Al elemental powders previously has been reported by Yu et al., 2010 [11], Samani et al., 2010 [12], Abbasi et al., 2010 [13], Krasnowski et al., 2007 [7], Enayati et al., 2004 [14], Lü et al., 1995 [15], Jang and Koch, 1990 [16].

However, there are still some uncertainty studies on the formation of Ni₃Al by MA processes such as effect of introduction of Fe contamination from milling media or air on its structure after milling. Characterization of nanocrystalline structure, morphology of powders and

*Corresponding author: Email: m.b.rahaei@gmail.com

purity of products is important in the development of these materials and as a means to control the quality of the synthesis.

On the other hand, Rietveld method has been becoming progressively popular for microstructural characterization of metallic and ceramic materials. It is common practice to estimate domain size, strain and lattice parameter values from the refined profile parameters [17-20].

Therefore, in this study the formation of nanocrystalline Ni₃Al intermetallic was investigated from Ni and Al elemental powders by mechanical alloying (MA) process. The alternations of the microstructure such as phase transformation, oxidation in air, grain size, microstrain, lattice parameter, morphology of particles and introduction of Fe impurity were evaluated after milling using XRD, Rietveld refinement, TEM, SEM, EDS and ICP analyses. Besides, XRD and Rietveld results were compared with TEM observations.

2. MATERIALS AND METHODS

2.1. Mechanical Alloying Process In this investigation, Ni (99.5% purity) and Al (99% purity) powders were used as starting materials. The Al particles had an irregular shape with a size distribution of 100–200 μm. Ni particles had nearly spherical morphology with a size distribution of 1 to 10 μm. Figs. 1a and b show scanning electron microscopy images in the secondary mode of the elemental powder particles for Al and Ni, respectively.

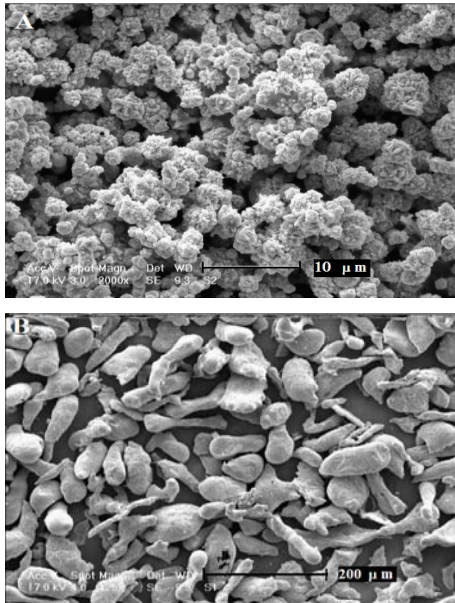


Fig. 1. SEM images of starting powder particles of: a. Ni and b. Al.

The ball mill used was a planetary mill that is classified as a high-energy ball mill. The milling media consisted of four 20 mm and three 14 mm diameter balls confined in a 150 ml volume vial. The material of ball and vial were hardened steel.

In all the experimental operations, Ni and Al powders with a composition of Ni₇₅Al₂₅ were mixed together and then milled for 1, 4, 8 and 16 under argon atmosphere. In all the MA runs, the ball-to-powder weight ratio (BPR) was set to 10:1 and milling speed was approximately 510 rpm. To prevent sample oxidation, the powders were sealed in the vial under the Ar atmosphere and a fresh sample was used for each ball milling run. Stearic acid (CH₃(CH₂)₁₆COOH) in the quantity of 2 wt% was utilized to avoid sticking of the powders to the vial and balls [21,22].

2.2. Structural Evolutions

2.2.1. XRD Analysis The structural evolution during milling was studied by X-ray diffractometer (XRD-Philips PW3710) with Cu K_α radiation (λ= 0.15406 nm) operating at 30 kV and 25 mA. Two-theta was recorded in the range of 20° and 80° with a step size of 0.02 (counting time was 2s per step at different polar tilting angles).

The lattice parameter of a cubic substance is directly proportional to the spacing 'd' of any particular set of lattice planes $a = d\sqrt{(h^2 + k^2 + l^2)}$ [23]. The Nelson-Riley method was used to minimize errors caused by aberration of 2θ variation and the lattice parameter 'a' of Ni₃Al was calculated for at least three peaks, using Eq. (1) [23,24].

$$F(\theta) = \frac{1}{2} \left(\frac{\cos^2 \theta}{\sin \theta} + \frac{\cos^2 \theta}{\theta} \right) \quad (1)$$

The Williamson–Hall method was used to evaluate the crystallite size using Eq. (2) [23,25]. This method is based on broadening of the diffraction lines due to the internal strain and crystallite size.

$$b \cos \theta = \frac{0.9\lambda}{d} + 2\varepsilon \sin \theta \quad (2)$$

Where 'θ' is the position of peak in the pattern (rad), 'D' is the crystallite size, 'ε' is the average micro strain in the powder, 'λ' is the wavelength of the radiation used (nm) and 'b' is the Full width at half maximum (FWHM) of the diffraction peak (rad). Silicon standard sample with large crystallites and free from defect broadening was used as a standard to increase the precision of the instrumental broadening similar in literature [23,26-28]. Then, the error of diffractometer was eliminated by Eq. (3) [23].

$$b = b_{size} + b_{strain} = \sqrt{b_o^2 - b_s^2} \quad (3)$$

Where ' b_s ' is the FWHM of the main peak of silicon standard sample ($2\theta = 28.5^\circ$) used for calibration and ' b_o ' is the FWHM of Ni_3Al 's peaks. Both ' b_s ' and ' b_o ' were calculated by X-Pert High Score software after automatic background removal.

The microstrain results in the present work were expressed as a root-mean-square 'r.m.s' microstrain, averaged over the distance $L \ll \epsilon_L^{-1/2}$, derived from the maximum microstrain ' ϵ ', with the assumption of a Gaussian microstrain distribution, by using Warren-Averbach method (Eq. (4)) [23,29].

$$\langle \epsilon_L^2 \rangle^{1/2} = \left(\frac{2}{\pi} \right)^{1/2} \epsilon \quad (4)$$

2.2.2. Rietveld Refinement Analysis

Microstructure characterization in terms of lattice parameter, grain size and r.m.s strain on milled products has also been evaluated using the Rietveld's refinement method in **materials analysis using diffraction** (MAUD, Version 2.26) software following the procedure indicated by Lutterotti [19,20].

In the Rietveld refinement, all of the data points of a powder pattern are fitted to structure models, which depend on adjustable parameters. The fitting to the measured XRD pattern is performed by a least-square calculation. The calculated curve is based on the crystallographic structure models, which also take into account the samples and instrumental effect. The parameters of this model are refined simultaneously to achieve the best fit to the data by least-square method. By least-square refinement describes the residual between calculated and measured data [17]:

$$R = \sum_i w_i [y_i(obs) - y_i(calc)]^2 \rightarrow \min$$

where R is the residual value of the merit function, w_i is $1/y_i(obs)$, $y_i(calc)$ denotes the calculated intensity and $y_i(obs)$ is the measured intensity at the i th step [17]. 2 θ correction, peak asymmetry and peak broadening parameters of a Si standard sample was assumed to have no size and strain broadening and were used as fitting and calibration parameters in MAUD software.

2.3. Microstructure Observations Microstructure observations of the morphology of selected mechanically alloyed powders were examined by a scanning electron microscope (SEM-Philips XL30) and transmission electron microscope (TEM-FEI-TECNAI G²). Crystal planes and lattice parameter were determined by measuring the ring radius of TEM micrograph.

2.4. Chemical Analysis Of Powders During Milling

The major goal of this test was to measure the actual

amount of iron contamination introduced during milling by both balls and vial. For this purpose, Inductivity Coupled Plasma-Atomic Emission Plasma (ICP-AES, ARL-3410) and Energy-Dispersive X ray Spectrometer (EDS) accompanied by the SEM were used. For EDS analyses, powders were coated with Au coating.

3. RESULTS AND DISCUSSION

3.1. X-Ray Diffraction Analysis Figure 2 indicates the XRD pattern of $Ni_{75}Al_{25}$ powder mixture after milling at different times. The XRD pattern of the milled powder for 1 h indicates the diffraction peaks of pure crystalline Ni and Al metals.

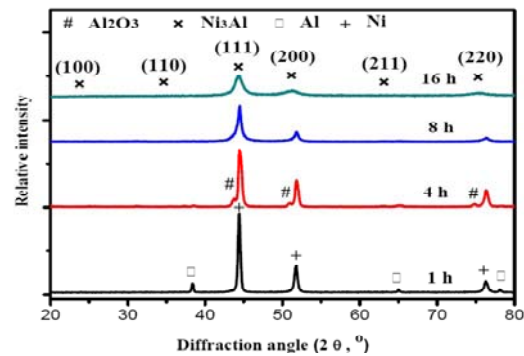


Fig. 2. XRD pattern of Ni and Al powders during milling.

After 4 h milling time opening vial in air atmosphere resulted in fast reaction of powders and firing (Figure 3). XRD pattern showed little Al_2O_3 phase along with Ni_3Al main phase. Due to high exothermic reaction between Ni and Al for obtaining Ni_3Al (153 KJ) [30], and Al for oxidation and formation of Al_2O_3 (1676 KJ) [31,32], it is logical to consider formation of Al_2O_3/Ni_3Al composite after opening vial of mechanical activated Ni and Al powders in air atmosphere.

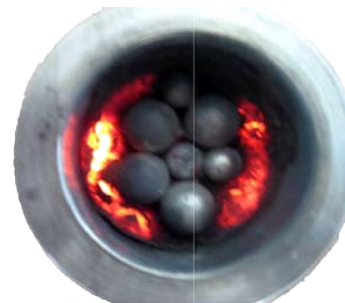


Fig. 3. Video output of the explosive reaction of 4 h milled powders after opening the container to the air.

Increasing milling time up to 8 h led to observation of Ni_3Al phase. Moreover, the XRD patterns indicated that no other intermediate phase was detected along

with Ni₃Al phase (Figure 2). Furthermore, opening vial in air atmosphere had no effect on Ni₃Al product since it is resistance to oxidation in air atmosphere at room temperature [32].

Enayati et al. [14] have attained Ni₃Al intermetallic almost after 20 and 40 h in RPM 390, BPR 6.5 and 3.25, respectively. Moreover, Yu et al. [11] obtained Ni₃Al after 40 h under RPM 500 and BPR 6 conditions. Also, Abbasi et al. [13] have reported obtaining Ni₃Al after 10 h milling time in BPR 20 and RPM 550. Developing of Ni₃Al at low milling time of 8 h is noticeable since the previous works reported the longer milling times for obtaining product. It is worth nothing that the time of complete transformation is unsteady and depends on some parameters such as ball to powder ratio, velocity of milling, etc. [6,10]. It seems that as the ball to powder ratio and milling speed increase, the time of attaining the Ni₃Al product decreases.

3.2. Structural Evolutions

3.2.1. Lattice Parameter The lattice parameter of Ni₃Al powder obtained from 8 and 16 h milling is calculated by Nelson-Riley equation (Eq. (1)) from the XRD analysis (Figure 4). In this method, the accurate lattice parameter is obtained by trend of function in zero content. Figure 4 shows that the lattice parameter decreases by increasing milling time. The refined XRD pattern of Ni₃Al sample milled for 16 h using MAUD software is shown in Figure 5 which is an example of profile fitting and separation of overlapping peaks.

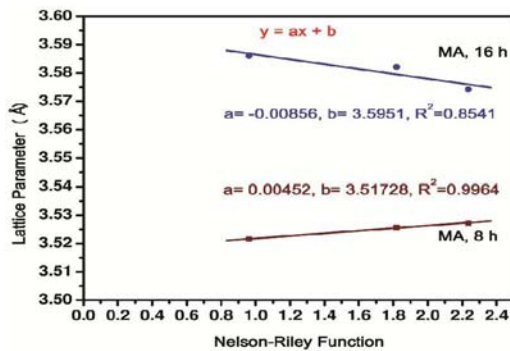


Fig. 4. Nelson–Riley function for obtaining the lattice parameter of Ni₃Al phase after 8 and 16 milling times.

The markers in Figure 5 are related to the experimental data and the solid lines show the calculated data using the Rietveld method. The residual curve (difference between the experimental and calculated data) is shown by the area under the curve (Figure 5).

As observed, there is a good agreement between the experimental and calculated spectra as the residual curve is negligible.

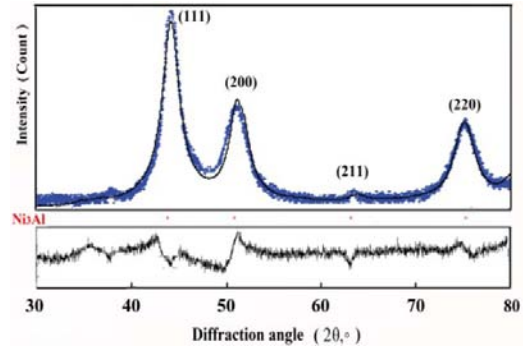


Fig. 5. Profile fitting of the Ni₃Al after 16 h milling in which the Pseudo–Voigt function is fitted.

The change of lattice parameter of milled samples for 8 and 16 h has presented in Table 1.

TABLE 1. The lattice parameter of Ni₃Al phase after 8 and 16 h milling times.

Milling time (h)	XRD, a (Å)	Rietveld, a (Å)
8	3.51728	3.5177
16	3.5951	3.5932

The lattice parameter increased a little during milling from 3.51 to 3.59 Å as measured by XRD analysis. XRD patterns gradually shifted towards lower angles (Figure 2), especially it was recognizable at 2θ 43.6° and subsequently increased the lattice parameter. As the Bragg law confirms, a decrease of the angle results in an increase of the lattice parameter [33].

Lattice parameter of powders during milling was compared with 00-009-0097 JCPDS reference code that it is 3.572 Å. In early stage of milling (8 h) the lattice parameters of Ni₃Al was lower than it's reference code. Lu et al. [15] and Abbasi et al. [13] have also obtained lower lattice parameter in early stage of milling for Ni₃Al intermetallic (≈ 3.51 Å). Moreover, Samani et al. [12] have obtained lower lattice parameter (≈ 3.52 Å) in Ni₃Al intermetallic with little impurity. Zhang [34] and Mhadhbi [35] proposed that the decrease of lattice parameter after milling should arise from the grain compression due to the presence of compressive stress fields within the non equilibrium grain boundaries inside of crystallites that results in the decrease of lattice parameter [35,36]. Suryanarayana [37] has reported that the decrease of lattice parameter is related to the vacancy-type defects in high enthalpy group of intermetallic compounds formed during milling.

In final stage of milling (16 h) the lattice parameters of Ni₃Al (≈ 3.59 Å) was higher than it's reference code. Samani et al. [12] have obtained higher lattice parameter of Ni₃Al (≈ 3.61 Å) similar to result of this research after 20 h milling with 1.42 wt% impurity of Fe. Pradhan et al. [38] have also obtained increasing lattice parameter from 3.52 Å to 3.58 Å by increasing

milling time. Suryanarayana [37] reported that lattice expansion or contraction is a natural consequence of disordering, which destroys the best packing of atoms realized in a completely ordered alloy. The magnitude of increase or decrease of the lattice parameter depends on the relative difference in the atomic size of the two components. It also depends on the relative difference in the atomic size of the constituent materials and the other elements or impurities which may have been introduced and dispersed in the lattice [37]. It is worth noting that in addition of vacancy or compressive stress during milling for change of lattice parameter, it seems Fe impurity from wearing out between balls, vial and powders has also an important factor for change of lattice parameter. So, it is valuable to investigate introduction of Fe impurity during milling.

3.2.2. Grain Size And Strain Evolutions By Williamson-Hall method crystallite size 'd' and strain 'ε' of milled powders were obtained (Figure 6).

As Figure 6 shows, increasing milling time up to 16 h led to increasing 'a' and decreasing of 'b' parameters of $y=ax+b$ function ($y=b \cos(\theta)$, $a=\epsilon$). The value of ϵ is the slope of $b \cos(\theta)$ function and the value of 'b' is obtained by extending the function in $2 \sin(\theta)=0$ content that results in obtaining of grain size ($d=0.9\lambda/b$). Increasing milling time up to 16 h led to increasing 'ε' and 'b' parameters. It means that strain increased and grain size decreased with increasing milling time. Results of Williamson-Hall (Figure 6) and Rietveld analysis techniques are reported in Table 2.

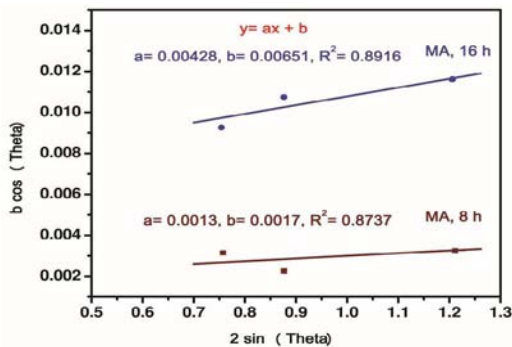


Fig. 6. Obtaining strain and crystallite size of Ni₃Al phase after 8 and 16 h milling times in accordance to Williamson-Hall equation.

TABLE 2. Crystallite size and r.m.s microstrain of Ni₃Al phase after 8 and 16 h milling times.

Milling time (h)	Methods	Grain Size (nm)	R.m.s Strain (%)
8	Williamson-Hall	81.6	0.1
	Rietveld	79	0.09
16	Williamson-Hall	21.3	0.34
	Rietveld	12.9	0.37

The data listed in the Table 2 suggest that the size of crystallites decreases rapidly from 81 to 21 nm and also

r.m.s microstrain increases from 0.1 to 0.34% in the product by increasing the milling time from 8 to 16 h. Thus, XRD and Rietveld refinement analyses confirmed each other about change of microstructure of products toward nano grain size. The formation of a nanostructured Ni₃Al during milling and consequently increase of hardness has confirmed by Jang and Koch [16], and Lü et. al. [15].

3.3. Morphology of Powders The morphology of the selected mechanically alloyed powders after milling for 1, 4, 8 and 16 h are shown in Figure 7.

Figure 7a indicates the average particle size of Ni and Al powders, which is the combination of the size of Al and Ni elemental powders after 1 h milling, separately. The morphology became more homogeneous, due to mixing both the elemental powders in this step and having the PCA.

The particles presented in Figure 7b are from the synthesized products after 4 h milling by oxidation in air including Ni₃Al and Al₂O₃ phases. Due to agglomeration of starting powders and synthesis in air, morphology of powders is in an inhomogeneous distribution of large and small sizes of particles in this stage.

By increasing milling time up to 8 h (Figure 7c), the morphology of powders changed to more homogenous along with little agglomeration. This event was occurred by the formation of a new Ni₃Al structure after the reaction between Ni and Al that was confirmed by the XRD pattern (Figure 2). Continuing milling time up to 16 h (Figure 7d), results in powders with an inhomogeneous morphology with high agglomeration. Then observations confirm a logical trend of increasing agglomeration in powders by increasing milling time up to this stage. The increase of agglomeration mechanism can be explained by increasing of cold weld of powders of Ni₃Al phase as a ductile system.

It seems continuing milling after 16 h repeats morphology of powders between 8 h and 16 h of milling condition and a steady state equilibrium is attained. Abbasi et al. [13] have reported that increasing milling time up to 55 h result in repeating fracture and cold-weld of powders almost in the same condition.

The mechanism of alloying involving two different ductile components system was suggested that in the early stages of MA, the attended particles get cold welded together and form a composite lamellar structure of the constituent metals. An increase in particle size is also observed at this stage. With increasing MA time, powder particles get work hardened, the hardness and consequently the brittleness increases, and the particles get fragmented resulting in particles with more equiaxed dimensions. Alloying begins to occur at this stage due to the combination of decreased diffusion distances (interlamellar spacing), increased lattice defect density, and any heating that may have occurred during milling

operation. The hardness and particle size tend to reach a saturation value at one stage, called the steady state processing stage [33].

For metallic and intermetallic powders, it is believed that fracturing and cold welding are not the major mechanisms for the grain size reduction [8]. Instead, the grain size reduction is due to the three other mechanisms: 1) localization of plastic deformation in the form of shear bands containing a high density of dislocations, 2) formation of subgrains or cells by annihilation of dislocations, and 3) the conversion of subgrains/cells into grains through mechanically driven grain rotation and subgrain boundary sliding [35,37].

3.4. EDS and ICP-AES Chemical Analyses of Powders during Milling

In order to further study of the chemical compositions of the milled powders and introduction of Fe, an EDS analysis of selected areas, as indicated in Figure 7, was performed with the results provided in Figure 8.

For a relatively short milling time of 1 h (Figure 8a), the detected Al content in powders (9.25 at. %) or other milling times it was lower than it's content in 3Ni-Al mixture (25 at. %). Due to heavy Ni element (58.69 g/mole) in comparison Al (26.98 g/mole), it was logical that EDS analysis showed small content of Al in the 3 Ni-Al mixture.

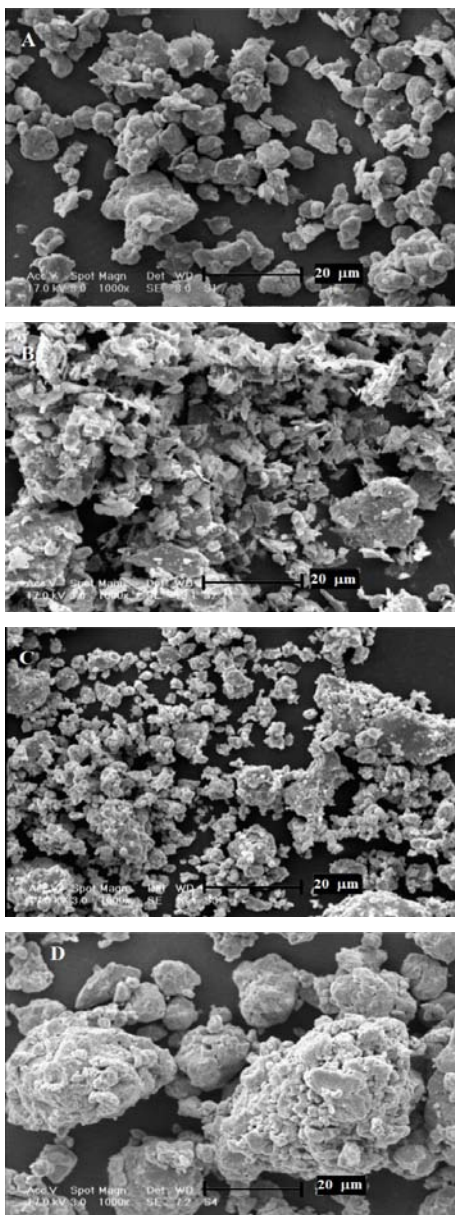


Fig. 7. SEM images of 3Ni-Al powders after different milling times × 1000: a. 1 h, b. 4 h, c. 8 h and d. 16 h.

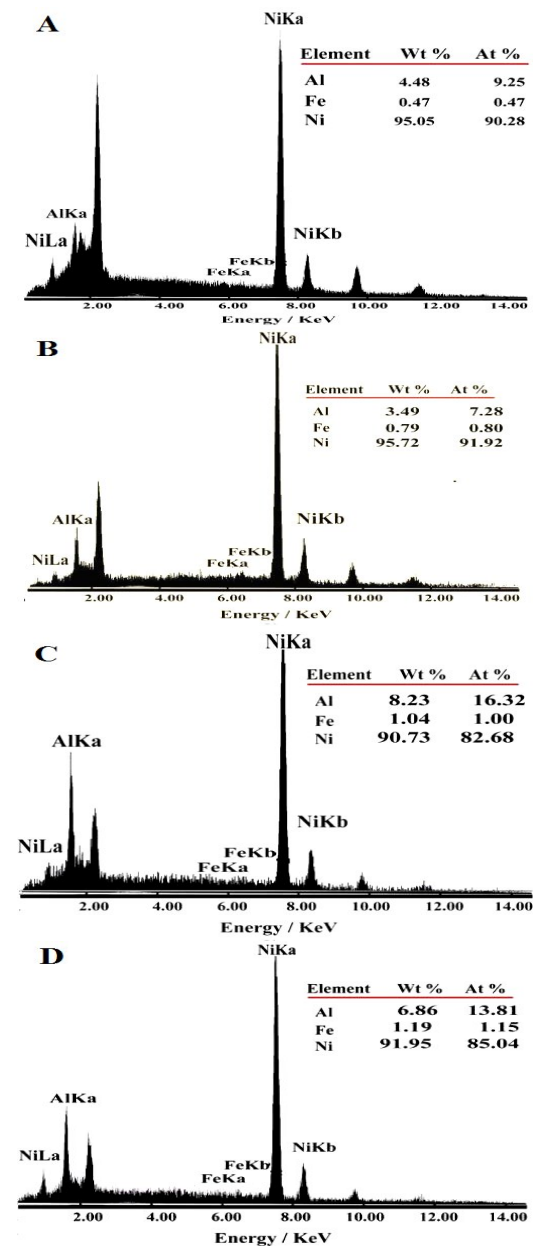


Fig. 8. EDS analysis of 3Ni-Al milled powders: a. 1 h, b. 4 h, c. 8 h and d. 16 h.

Besides, Fe debris was 0.47 wt% due to collision between the steel balls, vial and powders (Figure 8a). In addition, the EDS analysis of the Ni-Al mixture after 4 h milling detected Fe as an impurity in content of 0.79 wt% (Figure 8b). Moreover, the EDS analysis of the product powder after 8 and 16 h milling time showed increasing of Fe impurity in content of 1.04 wt% (Figure 7c) and 1.19 wt% (Figure 7d), respectively. However, it is reasonable to consider increasing of the Fe impurity mixed with the powders due to wearing out of the balls and powders with the vial during milling. Abbasi et al. [13] have also reported introduction of Fe impurity almost 8.45 at.% of Ni₃Al after 55 h milling.

Also, the Fe content in the starting materials and final product were measured using the ICP analysis, appreciating the accuracy of this test. The real Fe content in the Al and Ni starting materials were almost 0.42 wt% and 0 wt%, respectively. Moreover, Fe impurity after 16 h milling was 1.2 wt% by the ICP analysis. So, the Fe content in milling samples measured through the ICP was almost equal with EDS analysis and confirmed each other.

A flash back to the XRD pattern, presented in Figure 2, showed a little increase of the lattice parameter after 16 h milling with 1.2 wt% impurity of Fe that was similar to Samani et al. [12] results (after 20 h milling with 1.42 wt% Fe impurity). This phenomenon (increasing of lattice parameter by increasing milling time) can be interpreted as dissolving of Fe in the Ni₃Al structure since atomic radius of Fe is between radius of Ni and Al atoms [38]. Similar results about decrease or increase of lattice parameter of NiAl by introduction ternary element can be found in literature [39-41].

Figure 9 shows TEM images of nanostructured Ni₃Al after 16 h milling. Figure 9a and b show the bright field of Ni₃Al in different magnifications. Figure 9c and d show selected area diffraction (SAED) pattern of Ni₃Al from Figure 9a and b, respectively.

The size of grains was around 10-20 nm from TEM observation (Figure 9b) that confirmed XRD and Rietveld results for measuring grain size (21 & 13 nm) in Table 2. The lattice parameter was determined by measuring the ring radius and having camera constant in TEM analysis. The lattice parameter was measured almost 3.5949 Å (Figure 9c&d) which confirms the formation of Ni₃Al product and results of XRD and Rietveld analyses about increasing lattice parameter by increasing milling time.

Jang and Koch, 1990 [16] have shown that Ni₃Al structure tend to disorder (from comparison of the integrated intensity of the superlattice line (100) with that of the fundamental line (200) and amorphization by increasing milling time. Thus, it seems that there is obtained a disorder structure and nanocrystals of Ni₃Al embedded in an amorphous matrix after 16 h milling; since reflection planes related to the superlattice lines of Ni₃Al such as (100) and (110) are eliminated (Figure

2&9c) and reflection planes related to the fundamental lines of Ni₃Al such as (111), (200) and (220) are broadened, weakened or disappeared in TEM and XRD results after 16 h milling (Figure 2, 9c&d).

The formation of a full amorphous structure depends on compound properties, milling conditions and etc. [33]. It is worth noting that Suryanarayana [33] has presented that disorderity of structure in intermetallics causes to increase or decrease of their lattice parameter during milling. Therefore, increasing of lattice parameter can also be related to disordering and replacement of Ni and Al in Ni₃Al structure.

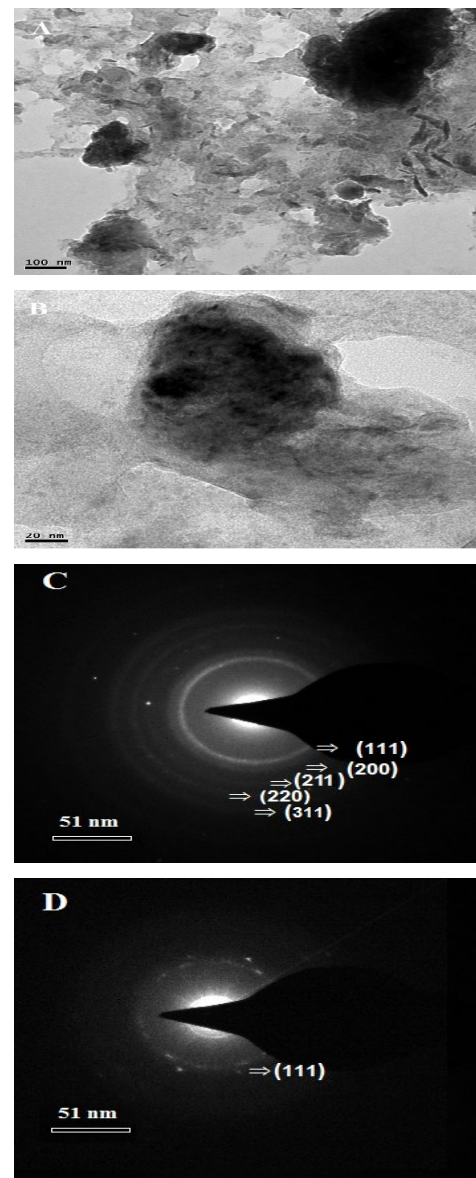


Fig. 9. TEM images of the Ni₃Al powder, a & b, Bright field images in different magnifications and c, d, their SAED patterns, respectively.

4. CONCLUSION

In this study, the production of nanostructured Ni₃Al powder from Ni and Al starting materials was evaluated by mechanical alloying process. After 4 h milling time opening vial in air atmosphere resulted in fast reaction of activated powders and formation Ni₃Al-Al₂O₃ composite.

Continuing milling time up to 8 h resulted in formation of Ni₃Al intermetallic confirmed by XRD analysis. In the early stage of milling (8 h) the lattice parameter of Ni₃Al (3.51 Å) was lower than its JCPDS reference code (3.572 Å). This can be related to the vacancy-type defect due to the high exothermic reaction during milling and the compressive stress on the materials between the balls and vial. TEM results confirmed both XRD and Rietveld analyses about obtaining a disorder structure and nanocrystals of Ni₃Al embedded in an amorphous matrix after 16 h milling. Increasing milling time up to 16 h also resulted in increasing the lattice parameter (3.59 Å) confirmed by XRD, Rietveld and TEM analyses that was probably caused by disordering in the Ni₃Al structure owing to the replacement of Ni and Al and/or dissolving the Fe impurity into the Ni₃Al structure due to wear of milling media and powders.

5. ACKNOWLEDGMENT

Corresponding author (Mohammad Bagher Rahaei) wishes to express his cordial gratitude to Prof. Dechang Jia in Institute for Advanced Ceramics, Harbin Institute of Technology (HIT), China for in part financial support and suitable suggestions for completion of this research.

6. REFERENCES

1. Stoloff, N. S., Liu, C. T. and Deevi, S. C., "Emerging applications of intermetallics", *Intermetallics*, Vol. 8, (2000), 1313-1320.
2. Garimella, N., Ode, M., Ikeda, M., Murakami, H. and Sohn, Y. H., "Effects of Ir or Ta alloying addition on interdiffusion of L12-Ni₃Al", *Intermetallics*, Vol. 16, (2008), 1095-1103.
3. Guo, J. T., Sheng, L. Y., Xie, Y., Zhang, Z. X., Ovcharenko, V. E. and Ye, H. Q., "Microstructure and mechanical properties of Ni₃Al and Ni₃Al-1B alloys fabricated by SHS/HE", *Intermetallics*, Vol. 19, (2011), 137-142.
4. Sikka, V. K., Deevi, S. C., Viswanathan, S., Swindeman, R. W. and Santella, M. L., "Advances in processing of Ni₃Al-based intermetallics and applications", *Intermetallics*, Vol. 8, (2000), 1329-1337.
5. Kordzadeh, E. and Bozorgmehr, M., "The effect of nickel increasing and aluminium addition on sulfidation resistance of Fe-Ni-Cr alloys", *International Journal of Engineering*, Vol. 21, (2008), 161-168.
6. Suryanarayana, C., "Mechanical alloying and milling", *Progress in Materials Science*, Vol. 46, (2001), 1-184.
7. Krasnowski, M., Antolak, A. and Kulik, T., "Nanocrystalline Ni₃Al alloy produced by mechanical alloying of nickel aluminides and hot-pressing consolidation", *Journal of Alloys and Compounds*, Vol. 434-435, (2007), 344-347.
8. El-Eskandarany, M. S., "Mechanical Alloying for Fabrication of Advanced Engineering Materials", William Andrew, Inc., New York, 2001.
9. Orban, R. L. and Lucaci, M., "Powder metallurgy impact on the nanocrystalline NiAl processing", *Romanian Journal of Physics*, Vol. 49, (2004), 885-892.
10. Takacs, L., "Self-sustaining reactions induced by ball milling", *Progress in Materials Science*, Vol. 47, (2002), 355-414.
11. Yu, Y., Zhou, J., Chen, J., Zhou, H., Guo, C. and Guo, B., "Synthesis of nanocrystalline Ni₃Al by mechanical alloying and its microstructural characterization", *Journal of Alloys and Compounds*, Vol. 498, (2010), 107-112.
12. Samani, M. N., Shokuhfar, A., Kamali, A. R. and Hadib, M., "Production of a nanocrystalline Ni₃Al-based alloy using mechanical alloying", *Journal of Alloys and Compounds*, Vol. 500, (2010), 30-33.
13. Abbasi, M., Sajjadi, S. A. and Azadbeh, M., "An investigation on the variations occurring during Ni₃Al powder formation by mechanical alloying technique", *Journal of Alloys and Compounds*, Vol. 497, (2010), 171-175.
14. Enayati, M. H., Sadeghian, Z., Salehi, M. and Saidi, A., "The effect of milling parameters on the synthesis of Ni₃Al intermetallic compound by mechanical alloying", *Materials Science and Engineering A*, Vol. 375-377, (2004), 809-811.
15. Lü, L., Lap, M.O. and Zhang, S., "Fabrication of Ni₃Al intermetallic compound using mechanical alloying technique", *Journal of Materials Processing Technology*, Vol. 48, (1995), 683-690.
16. Jang, J. S. C. and Koch, C. C., "Amorphization and disordering of the Ni₃Al ordered intermetallic by mechanical milling", *Journal of Materials Research Society*, Vol. 5, (1990), 498-510.
17. Young, R. A., "The Rietveld Method", 2nd ed., Oxford University Press, Inc., New York, 2002.
18. Dutta, H., Pradhan, S. K. and De, M., "Microstructural evolution on ball-milling elemental blends of Ni, Al and Ti by Rietveld's method", *Materials Chemistry and Physics*, Vol. 74, (2002), 167-176.
19. Lutterotti, L. and Gialanella, S., "X-ray diffraction characterization of heavily deformed metallic specimens", *Acta Materialia*, Vol. 46, (1998), 101-110.
20. Lutterotti, L., "MAUD Software", Version 2.26, (2010), <http://www.ing.unitn.it/~maud>.
21. Abasi Nargesi, F., Azari Khosroshahi, R. and Parvini Ahmadi, N., "Studying the effect of productive factors on synthesis of nanostructure TiAl (γ) alloy by mechanical alloying", *International Journal of Engineering*, Vol. 23, (2010), 147-156.
22. Abasi Nargesi, F., Azari Khosroshahi, R. and Parvini Ahmadi, N., "The influence of process control agent (P.C.A)'s state on expedition of mechanical alloying of nanostructure TiAl(γ) alloy", *International Journal of Engineering*, Vol. 23, (2010), 139-145.
23. Rahaei, M. B., Yazdani rad, R., Kazemzadeh, A. and Ebadzadeh, T., "Mechanochemical synthesis of nano TiC powder by mechanical milling of titanium and graphite powders", *Powder Technology*, Vol. 217, (2012), 369-376.
24. Razavi Tousi, S. S., Yazdani Rad, R., Rahimpour, M. R., Kazemzade, A. and Razavi, M., "Structural evolution of Al-20% (wt) Al₂O₃ system during ball milling stages", *International Journal of Engineering*, Vol. 22, (2009), 169-178.
25. Rahimpour, M. R. and Razavi, M., "Synthesis of TiC-Al₂O₃ nanocomposite from impure TiO₂ by mechanical activated sintering", *International Journal of Engineering*, Vol. 21, (2008), 275-280.
26. Bose, P., Bid, S., Pradhan, S. K., Pal, M. and Chakravorty, D., "X-ray characterization of nanocrystalline Ni₃Fe", *Journal of Alloys and Compounds*, Vol. 343, (2002), 192-198.
27. Ghosh, J., Chattopadhyay, S. K., Meikap, A. K. and Chatterjee, S. K., "Microstructure characterization of titanium-base aluminium alloys by X-ray diffraction using Warren-Averbach

- and Rietveld method", *Journal of Alloys and Compounds*, Vol. 453, (2008), 131–137.
28. Vives, S., Gaffet, E. and Meunier, C., "X-ray diffraction line profile analysis of iron ball milled powders", *Materials Science and Engineering A*, Vol. 366, (2004), 229–238.
 29. Djerdj, I. and Tonejc, A. M., "Structural investigations of nanocrystalline TiO₂ samples", *Journal of Alloys and Compounds*, Vol. 413, (2006), 159–174.
 30. Zhu, H., Ai, Y., Li, J., Min, J., Chu, D., Zhao, J. and Chen, J., "In situ fabrication of α -Al₂O₃ and Ni₂Al₃ reinforced aluminum matrix composites in an Al–Ni₂O₃ system", *Advanced Powder Technology*, Vol. 22, (2011), 629–633.
 31. Moussaa, S.O. and Morsi, K., "High-temperature oxidation of reactively processed nickel aluminide intermetallics", *Journal of Alloys and Compounds*, Vol. 426, (2006), 136–143.
 32. Cao, G., Geng, L., Zheng, Z. and Naka, M., "The oxidation of nanocrystalline Ni₃Al fabricated by mechanical alloying and spark plasma sintering", *Intermetallics*, Vol. 15, (2007), 1672–1677.
 33. Suryanarayana, C., "Mechanical Alloying and Milling", Marcel Dekker, Inc., New York, 2004.
 34. Zhang, D. L., "Processing of advanced materials using high-energy mechanical milling", *Progress in Materials Science*, Vol. 49, (2004), 537–560.
 35. Mhadhbi, M., Khitouni, M., Azabou, M. and Kolsi, A., "Characterization of Al and Fe nanosized powders synthesized by high energy mechanical milling", *Materials Characterization*, Vol. 59, (2008), 944–950.
 36. Zhang, K., Alexandrov, I. V. and Lu, K., "The X-ray diffraction study on a nanocrystalline Cu processed by equal-channel angular pressing", *Nanostructured Materials*, Vol. 9, (1997), 347–50.
 37. Pradhan, S. K., Shee, S. K., Chanda, A., Bose, P. and De, M., "X-ray studies on the kinetics of microstructural evolution of Ni₃Al synthesized by ball milling elemental powders", *Materials Chemistry and Physics*, Vol. 68, (2001), 166–174.
 38. Callister, W. D., "Fundamentals of Materials Science and Engineering", 7th ed., John Wiley & Sons, Inc., New York, 2007.
 39. Jiang, C., "Site preference of transition-metal elements in B2 NiAl: A comprehensive study", *Acta Materialia*, Vol. 55, (2007), 4799–4806.
 40. Schröpf, H., Kuhrt, C., Arzt, E. and Schultz, L., "Ordering versus disordering tendencies in mechanically alloyed (Ni_xFe_{1-x})Al alloys", *Scripta Metallurgica Materialia*, Vol. 30, (1994), 1569–1574.
 41. Andersona, I. M., Duncan, A. J. and Bentley, J., "Site-distributions of Fe alloying additions to B2-ordered NiAl", *Intermetallics*, Vol. 7, (1999), 1017–1024.

Synthesis and Characterization of Nanocrystalline Ni₃Al Intermetallic during Mechanical Alloying Process

R.Yazdani-rad, M. B. Rahaei*, A. Kazemzadeh, M. R. Hasanzadeh

Materials and Energy Research Center, Tehran, Iran

ARTICLE INFO

چکیده

Article history:

Received 5 March 2011

Received in revised form 5 February 2012

Accepted 19 April 2012

Keywords:

Ni₃Al
Mechanical alloying
Structural evolutions
Nanostructure
XRD
Rietveld refinement
TEM

در این تحقیق، تشکیل ترکیب بین فلزی نانوساختار Ni₃Al از پودرهای اولیه نیکل و آلومینیوم بوسیله فرآیند آلیاژسازی مکانیکی و مشخصه یابی آن بررسی شد. بنابراین، تغییر در ریز ساختار همچون استحاله فازی، اکسیداسیون در هوا و وارد شدن ناخالصی آهن از اجزاء آسیاب بعد از آسیاب با استفاده از پراش پرتو ایکس، هموارسازی ریتولد، میکروسکوپ الکترونی روبشی و عبوری، آنالیز عنصری و شیمیائی بررسی شدند. آسیاب پس از ۴ ساعت نتیجه در تشکیل کامپوزیت Ni₃Al/Al₂O₃ داد در حالی ادامه آسیاب تا ۸ ساعت نتیجه در تشکیل ترکیب Ni₃Al داد. مشاهدات TEM همراه با آنالیز پراش پرتو ایکس ترکیب شده با هموارسازی ریتولد به دست آوردن یک ساختار به سمت نامنظم و نانوکریستالهای Ni₃Al را در زمینه آمورف پس از ۱۶ ساعت تأیید کردند. علاوه بر این پارامتر شبکه و ناخالصی آهن با افزایش زمان آسیاب در محصول Ni₃Al افزایش یافت.

doi: 10.5829/idosi.ije.2012.25.02c.01